Discovery of a metastable $Al_{20}Sm_4$ phase

Z. Ye,[1,a)] F. Zhang,[1] Y. Sun,[1,2] M. I. Mendelev,[1] R. T. Ott,[1] E. Park,[1] M. F. Besser,[1] M. J. Kramer,[1] Z. Ding,[2] C.-Z. Wang,[1] and K.-M. Ho[1,2,3,a)]
[1]*Ames Laboratory, U.S. Department of Energy, Ames, Iowa 50011, USA*
[2]*Hefei National Laboratory for Physical Sciences at the Microscale and Department of Physics, University of Science and Technology of China, Hefei, Anhui 230026, China*
[3]*Department of Physics and Astronomy, Iowa State University, Ames, Iowa 50011, USA*

(Received 5 February 2015; accepted 26 February 2015; published online 9 March 2015)

We present an efficient genetic algorithm, integrated with experimental diffraction data, to solve a nanoscale metastable $Al_{20}Sm_4$ phase that evolves during crystallization of an amorphous magnetron sputtered $Al_{90}Sm_{10}$ alloy. The excellent match between calculated and experimental X-ray diffraction patterns confirms an accurate description of this metastable phase. Molecular dynamic simulations of crystal growth from the liquid phase predict the formation of disordered defects in the devitrified crystal. © *2015 AIP Publishing LLC*. [http://dx.doi.org/10.1063/1.4914399]

Non-equilibrium materials processing such as sputtering and melt spinning can give rise to a myriad of metastable structures. These unusual compounds in turn can have interesting properties. Rapidly solidified Al alloys containing rare earths and transition metals have attracted much attention due to their great mechanical properties including high tensile strengths and large strength-to-weight ratios.[1–4] The Al-Sm binary system is of particular interest because it provides a wide glass forming composition range and an array of metastable crystalline phases that are attainable from the liquid or the glass.[1,5,6] There has been considerable speculation between the short- and medium-range order in the as processed alloy and the formation of these metastable phases.[7] Yet such understanding is inhibited by detailed atomic descriptions of these metastable phases. Solving these far-from equilibrium crystalline structures is a big challenge due to their transient metastable nature, small grain sizes, and the fact they often contain disordered vacancies and anti-site defects. To overcome this challenge, we have recently developed an approach to solve complex crystal structures in far-from equilibrium transitions.[8] The approach effectively integrates lattice and space group information from X-ray diffraction (XRD) analysis with a genetic algorithm (GA) structural search,[9–13] followed by molecular dynamic (MD) simulations for crystal growth and Rietveld analysis to capture the distribution of defects in the system.

In this paper, we demonstrate that this methodology can be used to solve an unknown structure in a polyphased matrix of the metastable phases that evolve during devitrification of an amorphous sputtered $Al_{90}Sm_{10}$ alloy thin film. When the as-quenched amorphous thin film shown in Fig. 1(a) is isochronally heated, it separates into Al-rich and Al-poor amorphous regions at the early stage of annealing. Fcc-Al nanocrystals first precipitate in the Al-rich region, followed by a polyphased matrix of metastable phases, including Al_5Sm (Ref. 14) and an unknown phase, as shown in Fig. 1(b).

We first determine the unit cell from synchrotron XRD measurements using standard space group peak matching techniques. The unit cell is hexagonal with $a = 5.548$ Å, $c = 18.118$ Å. The estimated number of atoms per unit cell is around 25, assuming a density similar to the glass of 0.051 atoms/Å^3. As the compound is mixed with fcc-Al and Al_5Sm during the crystallization, its composition may differ from that of the amorphous alloy, i.e., Al with 10 at. % Sm. We performed a GA search for low-energy structures with a wide range of compositions, Al with 10–30 at. % Sm, and with the hexagonal unit cell determined by XRD. To expedite the GA search, a classical interatomic potential is used in the Finnis-Sinclair (FS) format[15] for energy calculations. As previously shown,[14,16] the FS potential, in general, gives a satisfactory estimation of the relative thermodynamic stability of the known stable and metastable phases. We then calculate the XRD pattern of each structure in the GA pool using the Rietveld program RIETAN-FP[17] and give a profile factor F_{XRD} by comparing calculated XRD to X-ray scattering experiments[7]

$$F_{XRD} = \sum_n \max(I_{n,cal}, I_{n,\exp}) \times \left(\log \frac{I_{n,cal}}{I_{n,\exp}}\right)^2. \quad (1)$$

The scatter plot of F_{XRD} versus the formation energy E_{form} is shown in Fig. 2(a) with the best structure in the pool marked

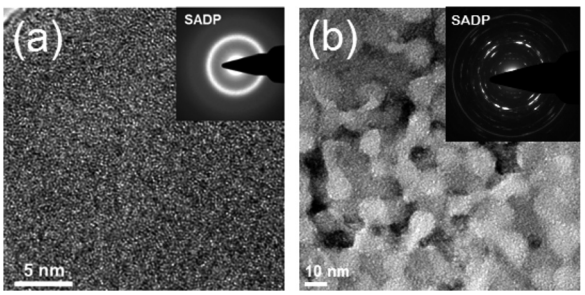

FIG. 1. (a) High-resolution transmission electron microscopy (HR TEM) image of as-quenched amorphous sputtered $Al_{90}Sm_{10}$ thin films. The inset shows the selected area diffraction pattern (SADP) that exhibits a featureless microstructure and a diffuse ring typical of an amorphous phase. (b) HR TEM image of a polyphased matrix of the metastable phases after heating to 425 K. The inset shows the corresponding SADP.

[a)]Authors to whom correspondence should be addressed: Electronic addresses: zye@iastate.edu and kmh@ameslab.gov

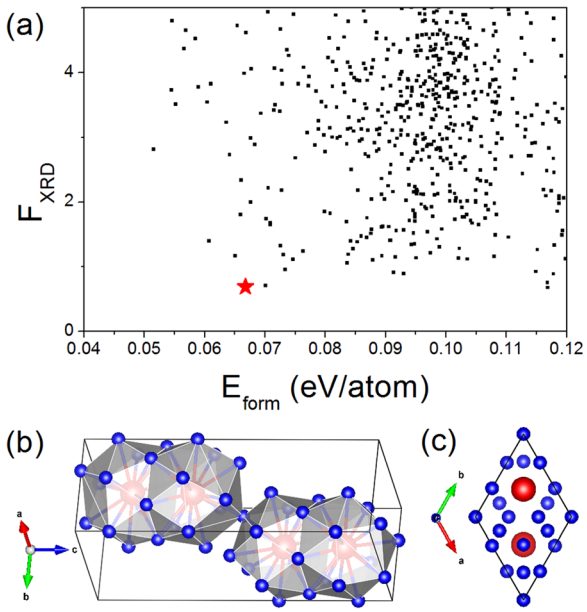

FIG. 2. (a) Scatter plot of the formation energy versus the profile factor with the best structure marked in star. (b) and (c) The structure of $Al_{20}Sm_4$. Blue (red) represents Al (Sm) atoms.

with star. Here, the best structure has the best (lowest) F_{XRD} and relatively low formation energy. Other structures have either a higher energy or a worse XRD profile. The formation energy is defined as the energy of an intermetallic phase with respect to the phase-separated mixture of fcc-Al and Al_3Sm

$$E_{form}(Al_xSm_y) = [E(Al_xSm_y) - (x-3y)E(Al) - yE(Al_3Sm)]/(x+y). \quad (2)$$

It has the stoichiometry $Al_{20}Sm_4$ with space group No. 182 ($P6_322$) with 5 Wyckoff positions. The structure is shown in Figs. 2(b) and 2(c). A more accurate DFT calculation shows that its formation energy at 0 K is 0.056 eV/atom.

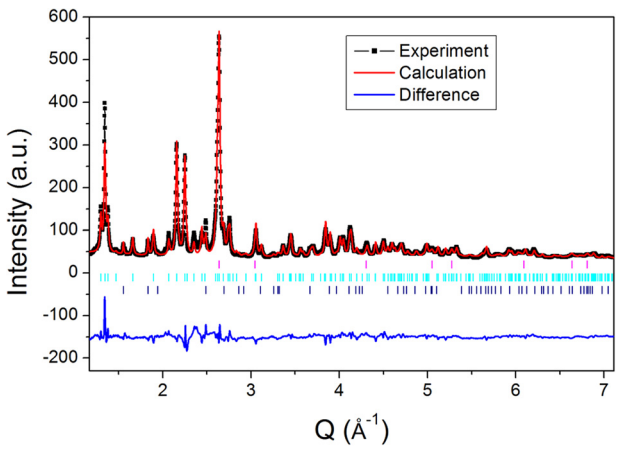

FIG. 3. Rietveld fitting of the XRD patterns for sputtered thin film Al-10%Sm sample at 550 K, showing the crystallization products of fcc Al, Al_5Sm, and the hexagonal $Al_{20}Sm_4$. The vertical lines in magenta, cyan, and navy show the diffraction peak positions for Al, $Al_{20}Sm_4$, and Al_5Sm, respectively. The fitting of the experimental data gives wRp = 0.079 and Rp = 0.0593, where wRp and Rp are the weighted and unweighted profile R-factors, respectively.[18]

A Rietveld fitting is done to refine the lattice, atomic positions, and site occupancies and compliments the DFT approach which cannot efficiently account for the many possible defect structures that can form. The fine time resolution of the XRD, 1 pattern per degree K, resulted in a one-to-one correspondence to the exothermic events observed in the differential scanning calorimeter (DSC), that is, from glass to a mixture of fcc-Al, Al_5Sm, and the hexagonal $Al_{20}Sm_4$ at 520 K, and from that to a mixture of fcc-Al, Al_5Sm (t), and Al_4Sm (o) at 575 K. We choose to fit the data at 550 K in the Rietveld refinement, which is in the middle of the stability range for the hexagonal phase. The result is shown in Fig. 3. The fitting of XRD pattern is comprised of three different phases: fcc-Al, Al_5Sm, and hexagonal Al20Sm4, which constitute ~12.1, 4.4, and 83.5 wt. %, respectively. The excellent match between the experimental and calculated XRD patterns confirms our prediction of the $Al_{20}Sm_4$ phase. Table I shows the lattice parameters and the atomic coordinates of the $Al_{20}Sm_4$ phase, given by both DFT calculations and the Rietveld analysis. However, the fitted phase fractions give an atomic composition of $Al_{86.6}Sm_{13.4}$, which is different from $Al_{90}Sm_{10}$ of the amorphous thin film. The Sm site being ~75% occupied gives a same wRp but a better atomic composition of $Al_{88.4}Sm_{11.6}$, indicating possible randomly distributed vacancies or anti-sites in the crystal.

While the crystal structure described above is in excellent agreement with the experimental XRD data, it does not really prove that it is realistic. It is well known that overfitting (i.e., fit to noise or experimental error by utilizing too many fitting parameters) can occur in the Rietveld analysis, which can lead to unphysical solutions of the structures. In particular, it is not clear whether the Sm site is fully occupied or ~75% partially occupied as suggested by the Rietveld fitting, since the partial occupancy only has a marginal improvement on the fitting. Neither it is clear whether the partial occupancy results from vacancies or Al-Sm antisites if the partial occupancy is true. To address these questions, we perform a large scale MD simulation to study the liquid-to-crystalline transformation. By studying the crystalline structure grown from liquid in the MD simulation, one can obtain a detailed description of the defects that are formed spontaneously within the grown crystal. In addition, the simulation provides information about the transformation pathway from amorphous to crystalline phase.

TABLE I. Lattice parameters and atomic coordinates of the $Al_{20}Sm_4$ phase with the space group No. 182 ($P6_322$). The numbers in parentheses are given by Rietveld analysis, and the rest by DFT calculations.

Lattice parameters (in unit of Å)				
a = 5.451 (5.548), c = 17.874 (18.118)				
Atomic coordinates				
	X	Y	Z	Multiplicities
Al1	0.345 (0.341)	0	0	6
Al2	0.333	0.667	0.119 (0.122)	4
Al3	0.166 (0.174)	0.332 (0.348)	0.25	6
Al4	0	0	0.615 (0.619)	4
Sm1	0.333	0.667	0.852 (0.851)	4

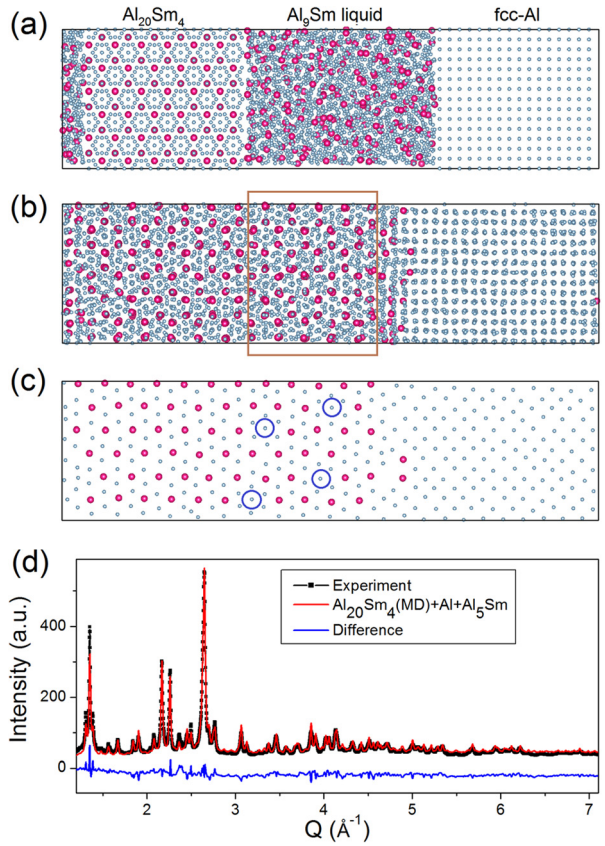

FIG. 4. (a) $Al_{20}Sm_4$ and fcc-Al crystal structures serve as seeds to grow crystalline structures from undercooled Al-10%Sm liquids (middle part). (b) The crystal structures are fully grown within 760 ns. (c) A slice of the structure in Fig. 4(b) shows anti-site defects marked in blue circles. (d) Fitting of the XRD pattern of the mixed 3 crystal structures: $Al_{20}Sm_4$ grown from MD simulations, fcc-Al and Al_5Sm.

Neglecting the small amount of Al_5Sm observed in the experiment, the initial model contains the liquid $Al_{90}Sm_{10}$ alloy sandwiched between the seeds of the perfect $Al_{20}Sm_4$ structure and fcc-Al (Fig. 4(a)). There is also a thin film of $Al_{90}Sm_{10}$ at the $Al_{20}Sm_4$/fcc-Al interface. The same classical potential that located at the $Al_{20}Sm_4$ structure is used since the MD simulation is beyond the spatial and temporal limits for *ab-initio* calculations. The simulation is performed at an elevated temperature of 800 K to expedite the transformation (the crystallization of this alloy is experimentally observed at ~520 K). The crystal structures are fully grown within 760 ns, as shown in Fig. 4(b). The Sm composition of the grown $Al_{20}Sm_4$ structure is ~14%, less than 16.7% of the perfect seed, indicating that the Sm site is indeed partially occupied. However, the occupancy of the Sm site in the grown hexagonal structure is ~84%, higher than ~75% predicted by the Rietveld analysis. A close look of the grown structure shows that some Sm sites are occupied by Al atoms, as indicated in Fig. 4(c). Fig. 4(d) shows the fitting of the XRD patterns for a mixture of fcc-Al, Al_5Sm, and the hexagonal $Al_{20}Sm_4$ structure grown from MD simulations as indicated in the brown frame in Fig. 4(b). We calculate the XRD patterns of the 3 crystal structures using the Mercury program.[19] Without fitting the atomic positions or site occupancies, we optimize the phase fraction, the lattice parameter, and the full width at half maximum with respect to experimental data. The fitting is similar to the one in Fig. 3, indicating a wide range of error in the site occupancies of the Rietveld fitting. Nevertheless, the large scale MD simulation provides a unique way to determine the site occupancies, along with a detailed picture of the defects in the crystal structure.

Both Rietveld analysis and MD simulations of crystal growth suggest that the $Al_{20}Sm_4$ structure contains a number of anti-site defects. It is thus interesting to calculate the formation energy of such defected structures to understand whether their structure stabilization is due to kinetic effects or to an entropy term. We calculated the formation energy of a structure with a single anti-site defect. The structure is created by substituting one Sm atom with Al in a $2 \times 2 \times 1$ supercell of $Al_{20}Sm_4$. The supercell is constructed to reduce the interaction between the defects. The 0 K formation energy with respect to fcc-Al and Al_3Sm of such a defected structure is 0.0563 eV/atom, very close to 0.0557 eV/atom of a structure without defects. The low formation energy of the anti-site defects suggests that the defects are stabilized by the entropical contribution at finite temperatures.

In summary, we search for an unknown meta-stable phase observed during the devitrification of Al-Sm glasses produced by magnetron sputtering using an efficient genetic algorithm. By combining GA and experimental diffraction data, we solved the phase with the stoichiometry $Al_{20}Sm_4$. The calculated X-ray diffraction spectrum matches excellently with that of the experiments. Rietveld refinements indicate that in the intermetallic compound the atomic sites have partial occupancies. Moreover, we perform MD simulations of the growth of this crystal phase from the liquid alloy and provide a realistic disordered structure that resembles the characteristics of the defects. The application of this combined experimental and computational approach has implications for understanding the phase competition/selection in highly driven systems.

We would like to thank Jon Almer for his assistance in the HEXRD experiments. Work at Ames Laboratory was supported by the U.S. Department of Energy, Basic Energy Sciences, Division of Materials Science and Engineering, under Contract No. DE-AC02-07CH11358, including a grant of computer time at the National Energy Research Supercomputing Center (NERSC) in Berkeley, CA. The high-energy X-ray experiments were performed at the XOR beamline (sector 1) of the Advanced Photon Source, Argonne National Laboratory, under Grant No. DE-AC02-06CH11357.

[1]A. Inoue, Prog. Mater. Sci. **43**, 365 (1998).
[2].Y. He, S. J. Poon, and G. J. Shiflet, Science **241**, 1640 (1988).
[3].H. S. Kim, P. J. Warren, B. Cantor, and H. R. Lee, Nanostruct. Mater. **11**, 241 (1999).
[4].Y. He, G. M. Dougherty, G. J. Shiflet, and S. J. Poon, Acta Metall. Mater. **41**, 337 (1993).
[5]J. Q. Guo, K. Ohtera, K. Kita, J. Nagohora, and N. S. Kazama, Mater. Lett. **24**, 133 (1995).
[6]Y. E. Kalay, C. Yeager, L. S. Chumbley, M. J. Kramer, and I. E. Anderson, J. Non-Cryst. Solids **356**, 1416 (2010).
[7]A. Inoue and A. Takeuchi, Mater. Sci. Eng., A **375–377**, 16 (2004).
[8]Z. Ye, F. Zhang, Y. Sun, M. C. Nguyen, M. I. Mendelev, R. T. Ott, E. S. Park, M. Besser, M. J. Kramer, Z.-J. Ding, C.-Z. Wang, and K.-M. Ho, "Unconventional phase selection in high-driven systems: A complex metastable structure prevails over simple stable phases," Proc. Nat. Acad. Sci. U.S.A. (submitted), preprint arXiv:1502.00023 (2015).
[9]D. M. Deaven and K. M. Ho, Phys. Rev. Lett. **75**, 288 (1995).

[10]M. Ji, C. Z. Wang, and K. M. Ho, Phys. Chem. Chem. Phys. **12**, 11617 (2010).
[11]M. Ji, K. Umemoto, C. Z. Wang, K. M. Ho, and R. M. Wentzcovitch, Phys. Rev. B **84**, 220105 (2011).
[12]X. Zhao, M. C. Nguyen, W. Zhang, C.-Z. Wang, M. J. Kramer, D. J. Sellmyer, X. Li, F. Zhang, L. Ke, V. P. Antropov, and K.-M. Ho, Phys. Rev. Lett. **112**, 045502 (2014).
[13]M. C. Nguyen, J. H. Choi, X. Zhao, C. Z. Wang, Z. Zhang, and K. M. Ho, Phys. Rev. Lett. **111**, 165502 (2013).
[14]F. Zhang, I. McBrearty, R. T. Ott, E. Park, M. I. Mendelev, M. J. Kramer, C.-Z. Wang, and K.-M. Ho, Scr. Mater. **81**, 32 (2014).
[15]M. W. Finnis and J. E. Sinclair, Philos. Mag. A **50**, 45 (1984).
[16]M. Mendelev, F. Zhang, Z. Ye, Y. Sun, M. Nguyen, S. Wilson, C. Z. Wang, and K. M. Ho, "Development of interatomic potentials appropriate for simulation of devitrification of $Al_{90}Sm_{10}$ alloy," Model. Simul. Mater. Sci. Eng. (submitted, 2014).
[17]F. Izumi and K. Momma, Solid State Phenom. **130**, 15–20 (2007).
[18] The Rietveld software package GSAS is used to fit the experiment XRD pattern. The definition of wRp and Rp can be found in the GSAS manual. https://subversion.xray.aps.anl.gov/EXPGUI/gsas/all/GSAS%20Manual.pdf (accessed Feb 25, 2015).
[19]Mercury - Crystal Structure Visualisation, Exploration and Analysis Made Easy. http://www.ccdc.cam.ac.uk/Solutions/CSDSystem/Pages/Mercury.aspx (accessed Feb 25, 2015).